





The global greening continues despite increased drought stress since 2000

Xin Chen ^a, Tiexi Chen ^{a b}  , Bin He ^c, Shuci Liu ^d, Shengjie Zhou ^a, Tingting Shi ^e

Show more 

 Outline |  Share  Cite

<https://doi.org/10.1016/j.gecco.2023.e02791> 

[Get rights and content](#) 

Under a Creative Commons [license](#) 

open access

Highlights

- The global greening is an indisputable fact.
- The rate of global greening increased slightly.
- The drought has only slowed the global greening, but not caused the global browning.

Abstract

Increases or decreases in remote sensing-based vegetation greenness are usually referred to as greening or browning. The CO₂ fertilization along with land management determined that greening is dominant. However, recently global browning signals due to drought stress have also been widely reported. In this study, We used the four latest leaf area index (LAI) datasets to explore this controversial topic, and found that global greening was not only present (trend between $3.1-6.4 \times 10^{-3} \text{ m}^2 \text{ m}^{-2} \text{ yr}^{-1}$) but also continued (growth rate trend between $3.3-6.4 \times 10^{-4} \text{ m}^2 \text{ m}^{-2} \text{ yr}^{-2}$) during 2001–2020. Greening acceleration occurred in 55.15% of the globe (positive trend and positive growth rate trend), while browning acceleration occurred in only 7.28% (negative trend and positive growth rate trend). Combined with meteorological variables, we found that CO₂ change dominated the LAI trend, while climate change largely determined the LAI growth rate trend. Importantly, our study highlighted that drought trend did not necessarily trigger vegetation browning, but slowed down the rate of greening.

Keywords

Leaf area index; Growth rate; Global greening; Climate change; Drought trend

1. Introduction

Vegetation is one of the basic components of terrestrial ecosystems and a regulator of climate change (Alkama et al., 2022, Griscom et al., 2017). Since the 1980s, the global leaf area index (LAI) based on satellite observations has shown a significant increasing trend, which is widely known as greening (Piao et al., 2020a). Numerous studies have confirmed the greening phenomenon, investigated the drivers and corresponding influences (Chen et al., 2019a, Chen et al., 2022b, Zhu et al., 2016). These studies found that global greening could reduce climate warming by increasing terrestrial carbon sequestration and cooling the surface (Chen et al., 2019b, Zeng et al., 2018).

However, the conclusion of greening has recently been challenged, with some studies finding that global greening stagnated or even turned browning after 2000 (Chen et al., 2022a, Liu et al., 2023, Pan et al., 2018, Yuan et al., 2019). Therefore, more and more attention has been paid to whether global vegetation is continuously greening or turning browning in recent years (Jiang et al., 2017, Wang et al., 2022). However, the results seem to be sensitive to the chosen datasets with different versions or sources. For example, Enhanced Vegetation Index (EVI) of MODIS showed opposite trends in version 5 and version 6 (Zhang et al., 2017). AVHRR-LAI illustrated global browning after 2000 (Chen et al., 2022a), which was in contrast to previous findings based on MODIS-LAI (Chen et al., 2019a).

The inconsistency of these findings has also led to widespread controversy among studies on the identification of key drivers. Studies supporting global browning primarily attribute browning to increased drought stress, and report potential mechanisms such as a sharp increase in atmospheric saturated vapor pressure difference (VPD) limiting vegetation growth (Yuan et al., 2019), excessive optimal temperatures inhibiting vegetation photosynthesis (Chen et al., 2022a), increasing water restriction on vegetation (Jiao et al., 2021), and reduced CO₂ fertilization effects due to water and nutrient availability (Wang et al., 2020). However, process-based models and observations suggest that global vegetation is still positively affected by CO₂ fertilization and land management, making greening dominant (Chen et al., 2019a, Zhu et al., 2016). These controversies not only increase the uncertainty in the estimation of global terrestrial carbon sources and sinks, but also hinder the better understanding of processes within terrestrial carbon cycle, which is of critically importance for the development of models to describe these processes.

Several key LAI datasets have been significantly updated recently, providing an opportunity to re-examine global vegetation change trends and their drivers over nearly two decades. The widely used GIMMS-LAI3g has been further updated to GIMMS-LAI4g, which solves a series of problems such as sensor drift (Cao et al., 2023). GLASS-LAI has also been updated to version 6, which shows higher accuracy compared to other products (Ma and Liang, 2022). The update of these products may help to reduce the uncertainty in the analysis of global vegetation change trends after 2000.

In addition, linear regression is often used to analyze the vegetation change trend in the current study. However, the vegetation change trend in the later period may be covered up in the case of widespread greening (or browning) in the earlier period (Pan et al., 2018). Some studies use piecewise linear regression

to characterize differences in vegetation change over different time periods, but this limits the application of some data sets with shorter time series (Chen et al., 2020, Wang et al., 2011). Therefore, another potential problem is how to determine a reliable indicator of whether the vegetation change trend has changed over a short period of time.

In order to explore these issues, in this study, we analyzed the global vegetation change trends from 2001 to 2020 based on the latest version of LAI datasets. Importantly, we also introduced the concept of LAI growth rate to analyze the rate of greening (browning). Finally, we further analyzed the drivers of LAI trend and LAI growth rate trend.

2. Method

2.1. Satellite data

LAI has clearer physical meaning compared to other vegetation greenness, which characterizes the area of green leaves on the ground (Fang et al., 2019). Therefore, we collected four widely used LAI datasets, including MODIS-LAI (C61), GLASS-LAI (V6), GIMMS-LAI4g (V1), and GLOBMap-LAI (V3), and these datasets are available during 2001–2020. MODIS-LAI is generated based on the spectral information of red band and near infrared band using look-up table (Knyazikhin et al., 1998). The spatial resolution of the dataset is 500m, and the temporal resolution is 8-day. GLASS-LAI is generated based on MODIS surface reflectance data using bidirectional long short-term memory model, and have high accuracy compared with observation (Ma and Liang, 2022). The spatial resolution of the dataset is 0.05° , and the temporal resolution is 8-day. GIMMS-LAI4g is generated based on PKU GIMMS NDVI product (data source from AVHRR and MODIS) and 3.6 million high-quality Landsat LAI samples using back propagation neural network, which eliminates the effects of satellite orbit drift and sensor degradation (Cao et al., 2023). The spatial resolution of this dataset is $1/12^\circ$, and the temporal resolution is half a month. GLOBMap-LAI is generated based on MODIS surface reflectance data using GLOBCARBON-LAI algorithm (Liu et al., 2012). The spatial resolution of this dataset is $1/13.75^\circ$, and the temporal resolution is half a month. In addition, we used the vegetation greenness dataset, including MODIS-NDVI (0.05° , 8-day), MODIS-EVI (0.05° , 8-day) and PKU GIMMS-NDVI ($1/12^\circ$, half month) (Li et al., 2023a) as auxiliary data to determine the global vegetation change trends. All pixels in each 0.5° grid cell with the center of each LAI and vegetation greenness datasets were averaged to 0.5° for global upscaling, and all data were aggregated to monthly scale to satisfy spatio-temporal consistency.

2.2. Meteorological data and CO₂ concentration data

Meteorological data were obtained from ERA5-land (Munoz-Sabater et al., 2021), and the selected variables included air temperature, precipitation, radiation, dew point temperature and surface soil moisture. The spatial resolution of these data is 0.1° , and the temporal resolution is monthly. To align with the LAI datasets, all pixels of meteorological data within 0.5° grid cell were upscaled. It is worth noting that VPD was not used in our study, although it is a very important meteorological driver for vegetation, we found that it has multicollinearity with other meteorological variables (the global average variance inflation factor was greater than 10), so in order to avoid covering up the contribution of other drivers to vegetation change, VPD was not used. The CO₂ concentration data were obtained from the CarbonTracker dataset (CT2022) with a spatial resolution of $3^\circ \times 2^\circ$ at monthly temporal scale (Jacobson et al., 2023), which was downsampled to 0.5° using nearest neighbor resample method.

2.3. Trend and growth rate trend

Trend that represent interannual changes in vegetation and meteorological variables at the global and grid scale were estimated using linear least squares and two-tailed t-test. In addition, we further estimated the growth rate of all data, a concept commonly applied to atmospheric CO₂ concentration (Keenan et al., 2016), which is used to represent the change rate of vegetation and meteorological variables, as follows:

$$Data_{gr} = Data_{t+1} - Data_t$$

where $Data_{gr}$ represents the growth rate and t represents a year from 2001 to 2020. The growth rate trends in time series were also analyzed. Therefore, there are four combinations of LAI: a positive trend with a positive growth rate trend (PP) indicates that greening is accelerating; a positive trend with a negative growth rate trend (PN) indicates that greening is slowing down; a negative trend with a positive growth rate trend (NP) indicates that browning is accelerating; a negative trend with a negative growth rate trend (NN) indicates that browning is slowing down.

2.4. Attribution analysis

Multiple linear regression model was used to quantify the contribution of all drivers to LAI trend and LAI growth rate trend, and this method has been widely used in quantifying the drivers of vegetation change trend (Jung et al., 2017, Li et al., 2023b, Song et al., 2022, Zou et al., 2023). Specifically, the meteorological variables, i.e., CO₂, air temperature (Airt), precipitation (P), radiation (Srad) and surface soil moisture (SM) were used as predictor variables and the LAI as well as the LAI growth rate as response variables. Taking the LAI trend as an example, the model can be expressed as

$$LAI_{obs} = \beta_{CO_2} \times CO_2 + \beta_{Airt} \times Airt + \beta_P \times P + \beta_{Srad} \times Srad + \beta_{SM} \times SM + \delta$$

where LAI_{obs} represents the LAI observed by the satellite during 2001–2020, β_{CO_2} , β_{Airt} , β_P , β_{Srad} and β_{SM} represent the sensitivity factors of CO₂, temperature, precipitation, radiation and soil moisture to LAI trend respectively, and δ is random error term. Therefore, the relative contribution of different drivers to the LAI trend can be obtained using the sensitivity factor multiplied by the interannual changes of different drivers, i.e

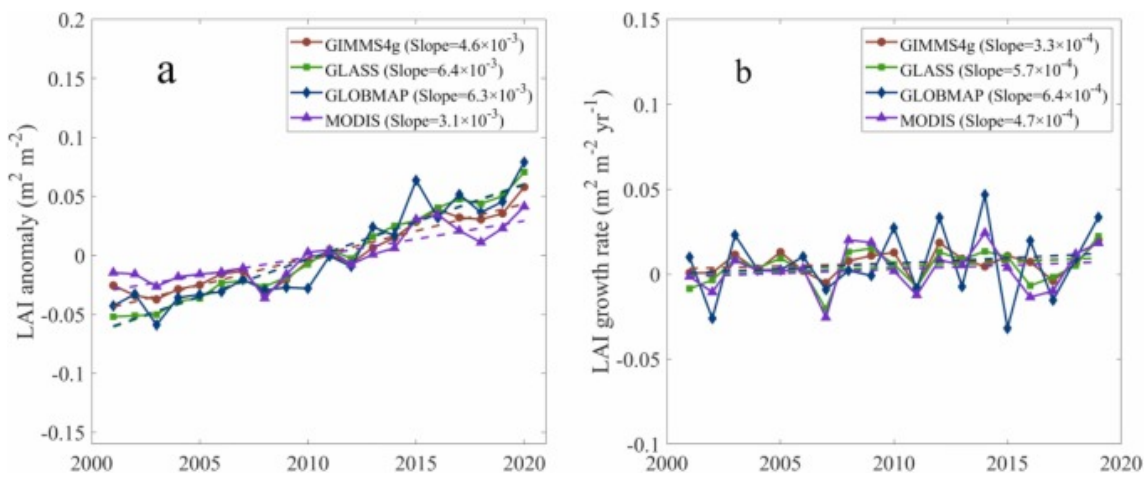
$$LAI_{obs} = LAI_{CO_2} + LAI_{Airt} + LAI_P + LAI_{Srad} + LAI_{SM} + \delta$$

where LAI_{CO_2} , LAI_{Airt} , LAI_P , LAI_{Srad} and LAI_{SM} represent the relative contributions of CO₂, temperature, precipitation, radiation and soil moisture to LAI trend, respectively. Similarly, we calculated the contribution of each driver to the LAI growth rate trend.

In order to reduce the uncertainty of multiple linear regression model in attribution analysis, we also used partial correlation analysis to identify the influence of different drivers on LAI trend and growth rate trend.

3. Result

All four LAI datasets showed significant global greening ($p < 0.05$) with a trend between $3.1 \times 10^{-3} \text{ m}^2 \text{ m}^{-2} \text{ yr}^{-1}$ and $6.4 \times 10^{-3} \text{ m}^2 \text{ m}^{-2} \text{ yr}^{-1}$ (Fig. 1a). Meanwhile, LAI growth rate showed a slight increasing trend with values between $3.3 \times 10^{-4} \text{ m}^2 \text{ m}^{-2} \text{ yr}^{-2}$ and $6.4 \times 10^{-4} \text{ m}^2 \text{ m}^{-2} \text{ yr}^{-2}$ (Fig. 1b), although none of them were significant ($p > 0.05$). Fig. S1 shows the change trend of vegetation greenness. Similar to LAI, NDVI and EVI also showed a significant increasing trend, and the growth rate was increasing. Therefore, at the globe scale, vegetation continued greening during 2001 - 2020.

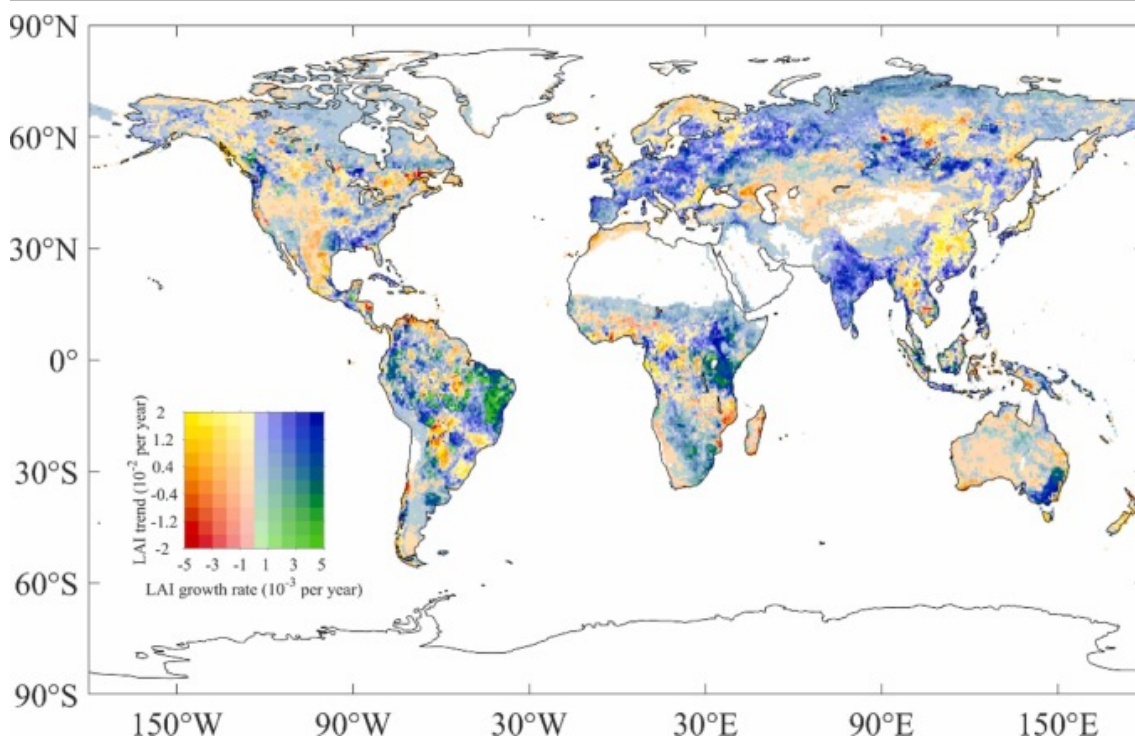


[Download : Download high-res image \(203KB\)](#)

[Download : Download full-size image](#)

Fig. 1. Trends (a) and growth rate trends (b) of four LAI datasets from 2001 to 2020.

The spatial pattern of LAI trend and LAI growth rate trend during 2001–2020 was further investigated. The distribution of trends was inconsistent between these datasets, especially in the tropical areas (Fig. S2). We counted areas with the consistent trend and growth rate trend in four LAI datasets. As shown in Fig. S3, 60.29% of the areas in the globe were inconsistent, however in the consistent areas, 64.06% (25.44%/39.71%) of the areas showed accelerated greening (PP group, see the method 2.3), mainly distributed in India, European plain and East Africa. The areas that browning was accelerating was only 2.07%, and most of them were distributed in Eastern area in Brazil. We further took the mean of the four data sets as a reference, and analyzed the trend and growth rate trend. As shown in Fig. 2, the greening was accelerating in 55.15% of the globe, among which the greening acceleration of India and European plains was the most obvious, while the greening of China and North America plains was slowing down. Only 14.44% of the globe was browning, with the accelerating (7.28%) and slowing down (7.16%) roughly equal.

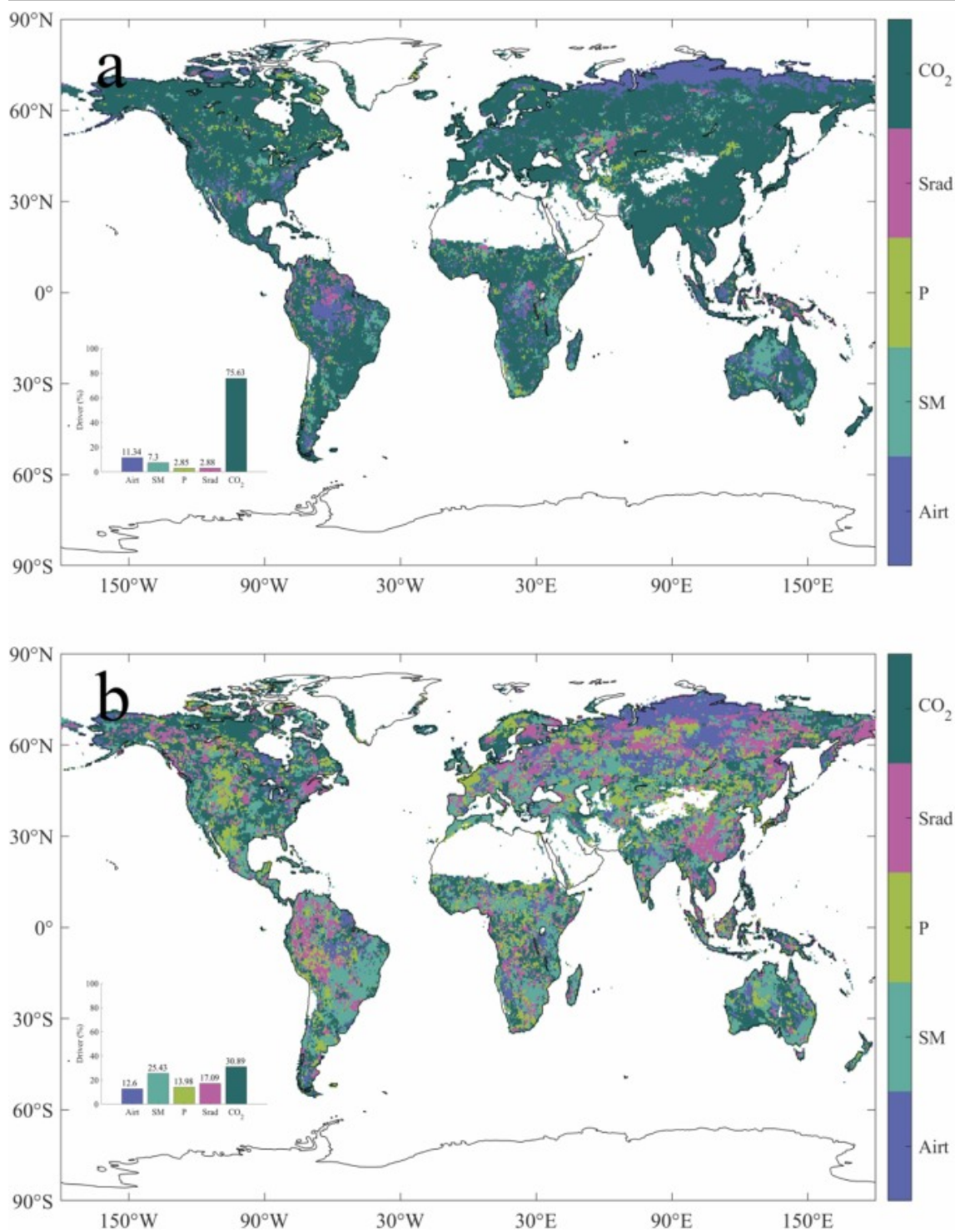


[Download : Download high-res image \(458KB\)](#)

[Download : Download full-size image](#)

Fig. 2. Spatial distribution of trend and growth rate trend based on the mean of four LAI datasets. Yellow and blue indicate that LAI shows a positive trend, yellow indicates a negative trend in LAI growth rate, and blue indicates a positive trend in LAI growth rate; Red and green indicate that LAI shows a negative trend, red indicates a negative trend in LAI growth rate, and green indicates a positive trend in LAI growth rate.

Multiple linear regression model could explain ($p < 0.05$) LAI trend and LAI growth rate trend in most areas of the globe, and the explanatory power of the model was generally poor in middle central Africa and high latitude regions such as northern North America (Fig. S4). Soil moisture led negative LAI trends in most areas of the globe, while temperature and CO₂ had positive contributions, especially in China, India and European plain (Fig. S5). In contrast, precipitation and radiation had almost no contribution to LAI trend. We further calculated the dominant drivers of LAI trend in each grid, and we found that CO₂ dominated the LAI trend of 75.63% of the globe, and temperature and soil moisture only could reach 11.34% and 7.30% respectively, which were mainly concentrated in the high latitude areas of the northern Hemisphere and western Australia. However, other meteorological factors could only dominate LAI trend in a few areas (Fig. 3a).



[Download : Download high-res image \(741KB\)](#)

[Download : Download full-size image](#)

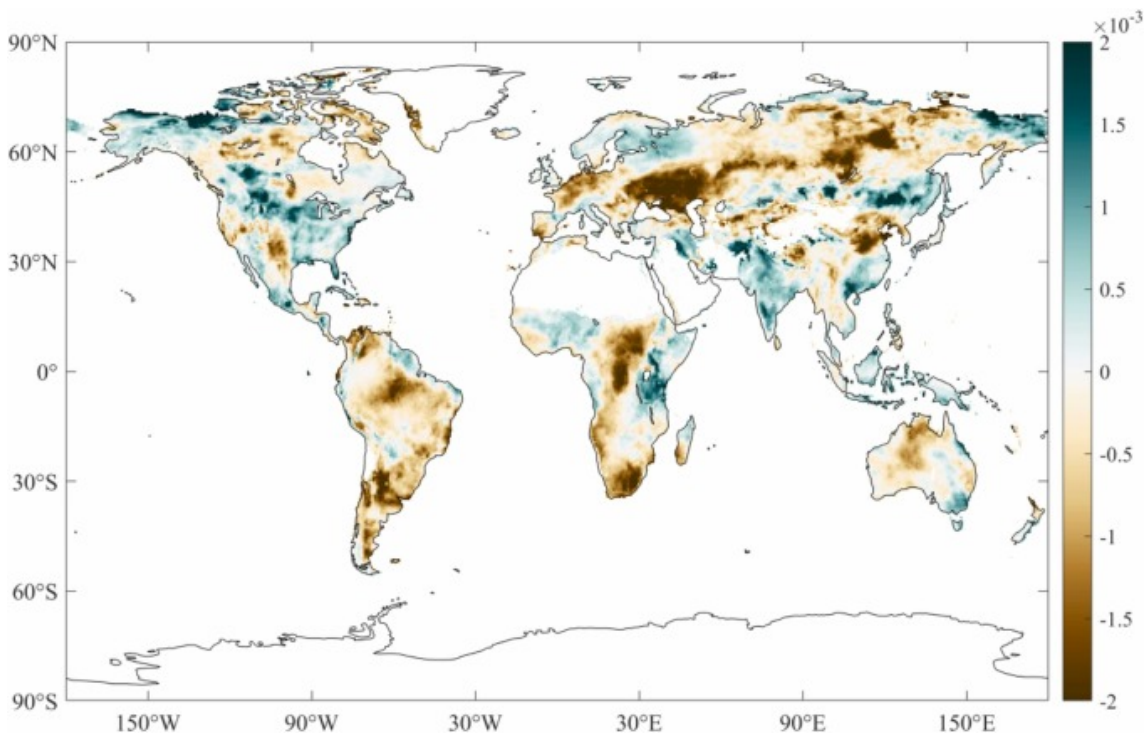
Fig. 3. Dominant drivers of LAI trend (a) and growth rate trend (b), defined as the drivers that contributed most to LAI trend or growth rate trend within each grid.

For the LAI growth rate trend, the contribution of each driver varied with regions without a clear spatial distribution rule (Fig. 3b). In general, soil moisture and radiation contributed more in most areas of the globe, with a significantly higher contribution of soil moisture than other drivers in areas such as the tropics and southeast Australia, and a very clear negative contribution of radiation in southern China (Fig. S6). In contrast, the contribution of temperature, precipitation and CO₂ to the LAI growth rate trend was relatively small in most areas. When we counted the dominant driver of each grid in the globe, we found that CO₂ could only dominate the LAI growth trend in 30.89% of areas, while the proportion of areas dominated by

meteorological factors increased significantly compare to their relative contribution to LAI trend, among which soil moisture and radiation reach 25.43% and 17.09% respectively.

Partial correlation analysis was used to further identify the dominant factors for LAI trend and growth rate trend at each grid in the globe. Similar to the results of multiple regression model, the spatial distribution of the two was roughly the same (Fig. S7). However, the areas dominated by CO₂ were all decreasing. The LAI trend was 39.54% and the growth rate trend was 11.56%, which was mainly caused by the differences in high latitudes in the northern Hemisphere. Partial correlation analysis suggested that the LAI trend and growth rate trend in this area were mainly dominated by air temperature and radiation.

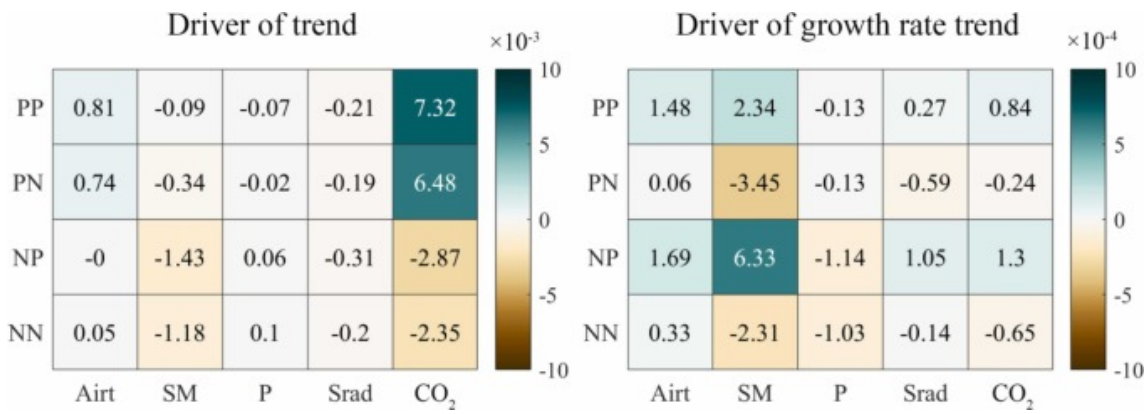
As a comprehensive index of temperature and precipitation, soil moisture can be used to measure the degree of dryness and wetness of an area. We noted a decreasing trend in soil moisture in most parts of the globe, indicating that drought stress had increased in recent years (Fig. 4). The globe was divided into four groups according to LAI trend and growth rate trend as suggested in the methods section, i.e., PP, PN, NP and NN. The soil moisture in the four sub-regions showed a decreasing trend, The trend of PP, PN, NP and NN were $-4.47 \times 10^{-4} \text{ m}^3 \text{ m}^{-3} \text{ yr}^{-1}$ ($p < 0.01$), $-3.57 \times 10^{-4} \text{ m}^3 \text{ m}^{-3} \text{ yr}^{-1}$ ($p < 0.01$), $-1.12 \times 10^{-4} \text{ m}^3 \text{ m}^{-3} \text{ yr}^{-1}$ ($p > 0.01$) and $-0.94 \times 10^{-4} \text{ m}^3 \text{ m}^{-3} \text{ yr}^{-1}$ ($p > 0.01$), respectively. We further calculated the LAI trend and growth rate trend of these four sub-regions. As shown in Fig. 5, similar to the results of the spatial analysis, soil moisture showed negative contributions to LAI trend in all sub-regions, indicating that drought trend seriously affected vegetation greening. In areas with positive LAI trend, the contribution of CO₂ (7.32×10^{-3} and 6.48×10^{-3}) was much higher than that of other drivers, making CO₂ dominant global greening. Compared with other drivers, soil moisture contributed more to the LAI growth rate trend, especially in NP and PN areas. In NP areas, soil moisture had positive contributions (6.33×10^{-4}), indicating that the changes of soil moisture contributed to the browning acceleration. On the contrary, soil moisture showed negative contributions (-3.45×10^{-4}) in PN areas, indicating that changes in soil moisture slowed down vegetation greening.



[Download : Download high-res image \(328KB\)](#)

[Download : Download full-size image](#)

Fig. 4. Spatial distribution of soil moisture trend from 2001 to 2020 (Unit: $\text{m}^3 \text{ m}^{-3} \text{ yr}^{-1}$).



Download : [Download high-res image \(168KB\)](#)

Download : [Download full-size image](#)

Fig. 5. Relative contributions of the drivers of LAI trend and growth rate trend in different areas. PP represents areas with positive LAI trend and positive growth rate trend, PN represents areas with positive LAI trend and negative growth rate trend, NP represents areas with negative LAI trend and positive growth rate trend, and NN represents areas with negative LAI trend and negative growth rate trend. Relative contributions were obtained by an area-weighted average of the contributions of drivers within different areas.

4. Discussions

4.1. Controversy on vegetation change trend after 2000

Earlier studies have confirmed the fact of global greening, but most of them considered the long-term trend since 1982, that is, all studies agree on global greening during 1982 – 2000 (Piao et al., 2020b, Zhu et al., 2016), however there is no widespread agreement on global greening after 2000 (Liu et al., 2023, Pan et al., 2018, Yuan et al., 2019). In this study, based on the latest remote sensing data, we try to answer the key question of whether the globe has been greening or browning since about 2000. Our results showed that the vegetation across the globe was greening and that the greening had maintained a slight acceleration (Fig. 1), which supports previous finding (Chen et al., 2019a). Therefore, the first thing that needs to be discussed here is the potential causes of the paradoxical phenomenon of global greening and global browning after 2000. The signal of the sensor used in the datasets is usually the first consideration. MODIS information is also used in the algorithm of the other three LAI datasets, which lead these datasets that we used are not absolutely independent. As we all know, MODIS sensors have long exceeded their designed service life, showing a series of problems such as sensor degradation in version 5 (Tian et al., 2015, Zhang et al., 2017). Fortunately, MODIS has been calibrated in subsequent versions, which greatly reduces the uncertainty of all kinds of datasets released. In addition, a study by Yan et al. (2021) confirmed the effectiveness of the MODIS calibration algorithm by comparing the LAI of MODIS with subsequent launched VIIRS, ruling out the possibility of false greening caused by sensor degradation.

In contrast, the global browning identified in most current studies is based on findings from AVHRR data sources (Chen et al., 2022a, Yuan et al., 2019), which should be used in caution. It is well known that AVHRR-based NDVI and LAI have multiple sources of uncertainty. There are obvious artificial signals from the orbital drift in the widely used GIMMS-NDVI3g and GIMMS-LAI3g based on AVHRR (Tian et al., 2015, Zhu et al., 2013). An important study by Wang et al. (2020) on the continued decline of the global CO₂ fertilization effect is also due to the fact that the quality of the AVHRR data source has also been widely questioned (Frankenberg et al., 2021, Zhu et al., 2021). Given that the global browning in GIMMS-NDVI3g and GIMMS-

LAI3g after 2000 translates into global greening in PKU GIMMS-NDVI and GIMMS-LAI4g after 2000 only due to algorithmic improvements and the addition of MODIS information, so one possible reason is that potential problems with AVHRR sensors trigger vegetation browning (Cao et al., 2023, Li et al., 2023a).

4.2. Indicators of the vegetation change rate

The introduction of the concept of LAI growth rate provides a new perspective for the analysis of global vegetation change and overcomes the limitations of traditional piecewise regression and breakpoint methods to a certain extent. Based on the LAI trend and LAI growth rate trend, we have some novel findings. Similar to the findings of Chen et al. (2019a), India and China were responsible for the overall global greening, but in terms of the rate of greening, the two countries showed opposite directions (Fig. 2). Greening was accelerating in India while it was slowing down in China, which has rarely been reported in previous studies. Multiple linear regression models attributed both phenomena to the effects of soil moisture, temperate and radiation, however it is clear that in China and India, two countries with significant land management, it is obviously impractical to attribute vegetation changes to meteorological factors alone. Therefore, another possible explanation is that different land management are responsible for the difference in the rate of greening. In China, after a massive afforestation program and agricultural modernization, greening may gradually reach saturation (Sha et al., 2022). And in India, irrigated agriculture, which mitigated atmospheric and soil drought and made vegetation less susceptible to moisture pressure, may have further enhanced greening (Ambika and Mishra, 2020).

4.3. The synergistic phenomenon of drought trend and greening

Without considering human activities, LAI trend is mainly determined by the positive effect of CO₂ fertilization and the negative effect of drought stress (Yuan et al., 2019, Zhu et al., 2016). A growing body of research shows that vegetation growth is enhanced by moisture constraints due to increased VPD and decreased soil moisture caused by climate warming (Jiao et al., 2021, Liu et al., 2020). However, It is not clear that the current drought trend reaches a threshold to exceed the positive effect of CO₂ fertilization. The introduction of the concept of growth rate provided additional explanation, as we found that the drought trend could only have a partial negative impact on vegetation, slowing down the vegetation greening and accelerating the vegetation browning. However, drought trend could not lead to global browning as it could not overtake the positive effect of CO₂ fertilization that contributed to global vegetation (Fig. 5). Our study explains the synergistic phenomenon of drought trends with greening, which is similar to recent findings on gross primary productivity, that is, the rise in VPD offsets only a small fraction of the increase in productivity caused by warming and CO₂, and gross primary productivity is still increasing globally (Song et al., 2022).

4.4. Limitations and prospects

In the attribution analysis of LAI trend and growth rate trend, there were some differences between multiple linear regression model and partial correlation analysis at high latitudes in the northern hemisphere. Partial correlation analysis showed that LAI trend and growth rate trend in this region were mainly affected by temperature and radiation, while multiple linear regression suggested that CO₂ was the dominant driver. The results of the partial correlation analysis seem more reasonable because some previous studies have shown that vegetation change in the high latitudes of the northern Hemisphere is mainly positively affected by climate warming (Berner et al., 2020, Keenan and Riley, 2018). Multiple linear regression model performed relatively poorly in this region and might not fully identify the contribution of individual drivers. In addition, our model does not include the contribution of land management, which has been highlighted in some previous studies (Chen et al., 2019a, Chen et al., 2022c, Chen et al., 2023). Of

course, the contribution of land management to LAI trend and growth rate trend may be implied in other drivers, such as the positive contribution of CO₂ to LAI trend in PP and PN areas.

Previous studies have demonstrated potential mechanisms by which different drivers affect LAI trend, such as climate warming promoting greening through lengthening the growing season in high latitudes (Keenan and Riley, 2018), CO₂ fertilization effects promoting LAI increase (Zhu et al., 2016), and afforestation and agricultural modernization leading to greening in China and India (Chen et al., 2019a). However, as for the LAI growth rate trend, this is a new concept. Although we have quantified the contribution of different drivers to the LAI growth rate trend on a global scale, there is no further study on its potential mechanism. In future studies, we can try to explore this problem, especially in China and India, two countries with opposite LAI growth rate trends.

5. Conclusion

In conclusion, based on the latest remote sensing data, we explored the important issue of global vegetation change trends after 2000. Importantly, we introduced the concept of growth rate to characterize the rate of greening/browning. Our results showed that the global greening was still present in 2001–2020, with 55.15% of areas greening at an accelerated rate, mainly concentrated in India and the European plains, compared with 7.28% of browning. Multiple linear regression and partial correlation analysis agreed that CO₂ dominated the LAI trend, while climate change determined the LAI growth rate trend. By analyzing different sub-regions of the globe, we found that the drought trend only slowed down global greening, but was far from triggering browning. These findings will improve our understanding of the processes within carbon cycle and narrow the research gap of better defining if the status of global vegetation is greening or browning in recent two decades.

CRedit authorship contribution statement

Liu Shuci: Validation, Writing – original draft. **He Bin:** Validation, Writing – original draft. **Chen Tiexi:** Conceptualization, Methodology, Validation, Visualization, Writing – original draft, Writing – review & editing. **Chen Xin:** Conceptualization, Data curation, Formal analysis, Methodology, Software, Validation, Writing – original draft, Writing – review & editing, Visualization. **Shi Tingting:** Validation, Writing – original draft. **Zhou Shengjie:** Validation, Writing – original draft.

Declaration of Competing Interest

The authors declare that they have no known competing financial interests or personal relationships that could have appeared to influence the work reported in this paper.

Acknowledgments

This study was supported by the National Natural Science Foundation of China (No. [42130506](#), [42161144003](#) and [31570464](#)) and the Postgraduate Research & Practice Innovation Program of Jiangsu Province (No. [KYCX23_1322](#)).

Author contributions

X.C. compiled the data, conducted analysis, prepared figures. X.C. and T.X.C. wrote the manuscript. X.C. and T.X.C. conceived the scientific ideas and designed this research. B.H., S.C.L, S.J.Z., and T.T.S. gave constructive suggestions for improving the manuscript.

Appendix A. Supplementary material

 [Download : Download Word document \(3MB\)](#)

Supplementary material

.

[Recommended articles](#)

Data Availability

Data will be made available on request.

References

[Alkama et al., 2022](#) R. Alkama, *et al.*

Vegetation-based climate mitigation in a warmer and greener World

Nat. Commun., 13 (1) (2022), Article 606

[View in Scopus ↗](#) [Google Scholar ↗](#)

[Ambika and Mishra, 2020](#) A.K. Ambika, V. Mishra

Substantial decline in atmospheric aridity due to irrigation in India

Environ. Res. Lett., 15 (12) (2020), Article 124060

[CrossRef ↗](#) [Google Scholar ↗](#)

[Berner et al., 2020](#) L.T. Berner, *et al.*

Summer warming explains widespread but not uniform greening in the Arctic tundra biome

Nat. Commun., 11 (1) (2020), Article 4621

[View in Scopus ↗](#) [Google Scholar ↗](#)

[Cao et al., 2023](#) S. Cao, *et al.*

Spatiotemporally consistent global dataset of the GIMMS leaf area index (GIMMS LAI4g) from 1982 to 2020

Earth Syst. Sci. Data, 15 (11) (2023), pp. 4877-4899

[CrossRef ↗](#) [View in Scopus ↗](#) [Google Scholar ↗](#)

[Chen et al., 2022a](#) B. Chen, *et al.*

Inhibitive Effects of Recent Exceeding Air Temperature Optima of Vegetation Productivity and Increasing Water Limitation on Photosynthesis Reversed Global Greening

Earth'S. Future, 10 (11) (2022), Article e2022EF002788

[View in Scopus ↗](#) [Google Scholar ↗](#)

[Chen et al., 2019a](#) C. Chen, *et al.*

China and India lead in greening of the world through land-use management

Nat. Sustain., 2 (2) (2019), pp. 122-129

[CrossRef ↗](#) [View in Scopus ↗](#) [Google Scholar ↗](#)

[Chen et al., 2019b](#) J.M. Chen, *et al.*

Vegetation structural change since 1981 significantly enhanced the terrestrial carbon sink

Nat. Commun., 10 (1) (2019), Article 4259

[View in Scopus](#) ↗ [Google Scholar](#) ↗

[Chen et al., 2020](#) T. Chen, *et al.*

The Greening and Wetting of the Sahel Have Levelled off since about 1999 in Relation to SST

Remote Sens., 12 (17) (2020), p. 2723

[CrossRef](#) ↗ [View in Scopus](#) ↗ [Google Scholar](#) ↗

[Chen et al., 2022b](#) T. Chen, *et al.*

Land Management Explains the Contrasting Greening Pattern Across China-Russia Border Based on Paired Land Use Experiment Approach

J. Geophys. Res.: Biogeosciences, 127 (6) (2022), Article e2021JG006659

[View in Scopus](#) ↗ [Google Scholar](#) ↗

[Chen et al., 2022c](#) T. Chen, *et al.*

Land Management Contributes significantly to observed Vegetation Browning in Syria during 2001-2018

Biogeosciences, 19 (5) (2022), pp. 1515-1525

[CrossRef](#) ↗ [Google Scholar](#) ↗

[Chen et al., 2023](#) X. Chen, A. Cai, R. Guo, C. Liang, Y. Li

Variation of gross primary productivity dominated by leaf area index in significantly greening area

J. Geogr. Sci., 33 (8) (2023), pp. 1747-1764

[Google Scholar](#) ↗

[Fang et al., 2019](#) H. Fang, F. Baret, S. Plummer, G. Schaepman-Strub

An overview of global leaf area index (LAI): methods, products, validation, and applications

Rev. Geophys., 57 (3) (2019), pp. 739-799

[CrossRef](#) ↗ [View in Scopus](#) ↗ [Google Scholar](#) ↗

[Frankenberg et al., 2021](#) C. Frankenberg, Y. Yin, B. Byrne, L. He, P. Gentine

Comment on "recent global decline of CO₂ fertilization effects on vegetation photosynthesis" COMMENT

Science, 373 (6562) (2021)

[Google Scholar](#) ↗

[Griscom et al., 2017](#) B.W. Griscom, *et al.*

Natural climate solutions

Proc. Natl. Acad. Sci. USA, 114 (44) (2017), pp. 11645-11650

[CrossRef](#) ↗ [View in Scopus](#) ↗ [Google Scholar](#) ↗

[Jacobson et al., 2023](#) Jacobson, A.R. *et al.*, 2023. CarbonTracker CT2022. NOAA Global Monitoring Laboratory.

[Google Scholar](#) ↗

[Jiang et al., 2017](#) C. Jiang, *et al.*

Inconsistencies of interannual variability and trends in long-term satellite leaf area index products

Glob. Change Biol., 23 (10) (2017), pp. 4133-4146

[CrossRef ↗](#) [View in Scopus ↗](#) [Google Scholar ↗](#)

[Jiao et al., 2021](#) W. Jiao, *et al.*

Observed increasing water constraint on vegetation growth over the last three decades

Nat. Commun., 12 (1) (2021), Article 3777

[View in Scopus ↗](#) [Google Scholar ↗](#)

[Jung et al., 2017](#) M. Jung, *et al.*

Compensatory water effects link yearly global land CO₂ sink changes to temperature

Nature, 541 (7638) (2017), pp. 516-520

[CrossRef ↗](#) [View in Scopus ↗](#) [Google Scholar ↗](#)

[Keenan et al., 2016](#) T.F. Keenan, *et al.*

Recent pause in the growth rate of atmospheric CO₂ due to enhanced terrestrial carbon uptake

Nat. Commun., 7 (1) (2016), Article 13428

[View in Scopus ↗](#) [Google Scholar ↗](#)

[Keenan and Riley, 2018](#) T.F. Keenan, W.J. Riley

Greening of the land surface in the world's cold regions consistent with recent warming

Nat. Clim. Change, 8 (9) (2018), pp. 825-828

[CrossRef ↗](#) [View in Scopus ↗](#) [Google Scholar ↗](#)

[Knyazikhin et al., 1998](#) Y. Knyazikhin, J.V. Martonchik, R.B. Myneni, D.J. Diner, S.W. Running

Synergistic algorithm for estimating vegetation canopy leaf area index and fraction of absorbed photosynthetically active radiation from MODIS and MISR data

J. Geophys. Res.: Atmos., 103 (D24) (1998), pp. 32257-32275

[View in Scopus ↗](#) [Google Scholar ↗](#)

[Li et al., 2023a](#) M. Li, *et al.*

Spatiotemporally consistent global dataset of the gimms normalized difference vegetation index (PKU GIMMS NDVI) from 1982 to 2022

Earth Syst. Sci. Data, 15 (9) (2023), pp. 4181-4203

[CrossRef ↗](#) [View in Scopus ↗](#) [Google Scholar ↗](#)

[Li et al., 2023b](#) S. Li, *et al.*

Vegetation growth due to CO₂ fertilization is threatened by increasing vapor pressure deficit

J. Hydrol., 619 (2023), Article 129292

 [View PDF](#) [View article](#) [View in Scopus ↗](#) [Google Scholar ↗](#)

[Liu et al., 2020](#) L. Liu, *et al.*

Soil moisture dominates dryness stress on ecosystem production globally

Nat. Commun., 11 (1) (2020), Article 4892

[View in Scopus ↗](#) [Google Scholar ↗](#)

[Liu et al., 2023](#) Q. Liu, *et al.*

Vegetation browning: global drivers, impacts, and feedbacks

Trends Plant Sci., 28 (9) (2023), pp. 1014-1032

 [View PDF](#) [View article](#) [View in Scopus ↗](#) [Google Scholar ↗](#)

[Liu et al., 2012](#) Y. Liu, R. Liu, J.M. Chen

Retrospective retrieval of long-term consistent global leaf area index (1981–2011) from combined AVHRR and MODIS data

J. Geophys. Res.: Biogeosciences, 117 (G4) (2012)

[Google Scholar ↗](#)

[Ma and Liang, 2022](#) H. Ma, S. Liang

Development of the GLASS 250-m leaf area index product (version 6) from MODIS data using the bidirectional LSTM deep learning model

Remote Sens. Environ., 273 (2022), Article 112985

 [View PDF](#) [View article](#) [View in Scopus ↗](#) [Google Scholar ↗](#)

[Munoz-Sabater et al., 2021](#) J. Munoz-Sabater, *et al.*

ERA5-Land: a state-of-the-art global reanalysis dataset for land applications

Earth Syst. Sci. Data, 13 (9) (2021), pp. 4349-4383

[CrossRef ↗](#) [View in Scopus ↗](#) [Google Scholar ↗](#)

[Pan et al., 2018](#) N. Pan, *et al.*

Increasing global vegetation browning hidden in overall vegetation greening: Insights from time-varying trends

Remote Sens. Environ., 214 (2018), pp. 59-72

 [View PDF](#) [View article](#) [View in Scopus ↗](#) [Google Scholar ↗](#)

[Piao et al., 2020a](#) S. Piao, *et al.*

Characteristics, drivers and feedbacks of global greening

Nat. Rev. Earth Environ., 1 (1) (2020), pp. 14-27

[View in Scopus ↗](#) [Google Scholar ↗](#)

[Piao et al., 2020b](#) S. Piao, *et al.*

Interannual variation of terrestrial carbon cycle: Issues and perspectives

Glob. Change Biol., 26 (1) (2020), pp. 300-318

[CrossRef ↗](#) [View in Scopus ↗](#) [Google Scholar ↗](#)

[Sha et al., 2022](#) Z. Sha, *et al.*

The global carbon sink potential of terrestrial vegetation can be increased substantially by optimal land management

Commun. Earth Environ., 3 (1) (2022), p. 8

[View in Scopus ↗](#) [Google Scholar ↗](#)

[Song et al., 2022](#) Y. Song, W. Jiao, J. Wang, L. Wang

Increased global vegetation productivity despite rising atmospheric dryness over the last two decades

Earth'S. Future, 10 (7) (2022), Article e2021EF002634

[View in Scopus ↗](#) [Google Scholar ↗](#)

[Tian et al., 2015](#) F. Tian, *et al.*

Evaluating temporal consistency of long-term global NDVI datasets for trend analysis

Remote Sens. Environ., 163 (2015), pp. 326-340

 [View PDF](#) [View article](#) [View in Scopus ↗](#) [Google Scholar ↗](#)

[Wang et al., 2020](#) S. Wang, *et al.*

Recent global decline of CO₂ fertilization effects on vegetation photosynthesis

Science, 370 (6522) (2020)

1295-+

[Google Scholar ↗](#)

[Wang et al., 2011](#) X. Wang, *et al.*

Spring temperature change and its implication in the change of vegetation growth in North America from 1982 to 2006

Proc. Natl. Acad. Sci. USA, 108 (4) (2011), pp. 1240-1245

[CrossRef ↗](#) [View in Scopus ↗](#) [Google Scholar ↗](#)

[Wang et al., 2022](#) Z. Wang, *et al.*

Large discrepancies of global greening: indication of multi-source remote sensing data

Glob. Ecol. Conserv., 34 (2022), Article e02016

 [View PDF](#) [View article](#) [View in Scopus ↗](#) [Google Scholar ↗](#)

[Yan et al., 2021](#) K. Yan, *et al.*

Performance stability of the MODIS and VIIRS LAI algorithms inferred from analysis of long time series of products

Remote Sens. Environ., 260 (2021), Article 112438

 [View PDF](#) [View article](#) [View in Scopus ↗](#) [Google Scholar ↗](#)

[Yuan et al., 2019](#) W. Yuan, *et al.*

Increased atmospheric vapor pressure deficit reduces global vegetation growth

Sci. Adv., 5 (8) (2019), p. eaax1396

[View in Scopus ↗](#) [Google Scholar ↗](#)

[Zeng et al., 2018](#) Z. Zeng, L. Peng, S. Piao

Response of terrestrial evapotranspiration to Earth's greening

Curr. Opin. Environ. Sustain., 33 (2018), pp. 9-25

 [View PDF](#) [View article](#) [View in Scopus ↗](#) [Google Scholar ↗](#)

[Zhang et al., 2017](#) Y. Zhang, C. Song, L.E. Band, G. Sun, J. Li

Reanalysis of global terrestrial vegetation trends from MODIS products: browning or greening?

Remote Sens. Environ., 191 (2017), pp. 145-155

 [View PDF](#) [View article](#) [View in Scopus ↗](#) [Google Scholar ↗](#)

[Zhu et al., 2013](#) Z. Zhu, *et al.*

Global data sets of vegetation leaf area index (LAI)_{3g} and fraction of photosynthetically active radiation (FPAR)_{3g} derived from global inventory modeling and mapping studies (GIMMS) normalized difference vegetation index (NDVI_{3g}) for the period 1981 to 2011
Remote Sens., 5 (2) (2013), pp. 927-948

[CrossRef ↗](#) [View in Scopus ↗](#) [Google Scholar ↗](#)

[Zhu et al., 2016](#) Z. Zhu, *et al.*

Greening of the earth and its drivers

Nat. Clim. Change, 6 (8) (2016), pp. 791-795

[CrossRef ↗](#) [View in Scopus ↗](#) [Google Scholar ↗](#)

[Zhu et al., 2021](#) Z. Zhu, *et al.*

Comment on "Recent global decline of CO₂ fertilization effects on vegetation photosynthesis" COMMENT

Science, 373 (6562) (2021)

[Google Scholar ↗](#)

[Zou et al., 2023](#) L. Zou, K. Stan, S. Cao, Z. Zhu

Dynamic global vegetation models may not capture the dynamics of the leaf area index in the tropical rainforests: a data-model intercomparison

Agric. For. Meteorol., 339 (2023), Article 109562

 [View PDF](#) [View article](#) [View in Scopus ↗](#) [Google Scholar ↗](#)

Cited by (0)

© 2023 The Author(s). Published by Elsevier B.V.



All content on this site: Copyright © 2024 Elsevier B.V., its licensors, and contributors. All rights are reserved, including those for text and data mining, AI training, and similar technologies. For all open access content, the Creative Commons licensing terms apply.

